Supplement of

Spatial and temporal distribution of fine aerosol acidity in the Eastern Mediterranean

Neroladaki et al.

A1. Summary of the studied sites

Table S1: Characteristics of the sites used in this study. A brief description of each site which took place in the PANACEA campaigns can be found here https://panacea-ri.gr/index.php/observational-facilities/?lang=en. Coordinates in WGS84.

Site	Site – Full Name	Latitude (N)	Longitude (E)	Altitude (m a.s.l)	Site characteristic
FKL	Finokalia	35.33°	25.67°	250	coastal, background
THI	Thissio	37.97°	23.72°	105	urban background
PTR	Patra	38.30°	21.81°	100	urban background
IOA	Ioannina	39.65°	20.85°	518	urban background
LAP	Thessaloniki	40.63°	22.95°	50	urban
XAN	Xanthi	41.15°	24.92°	75	suburban background, rural

A2. Timeseries of Temperature and Relative Humidity measurements at the 6 sites during winter 2020 and summer 2019.
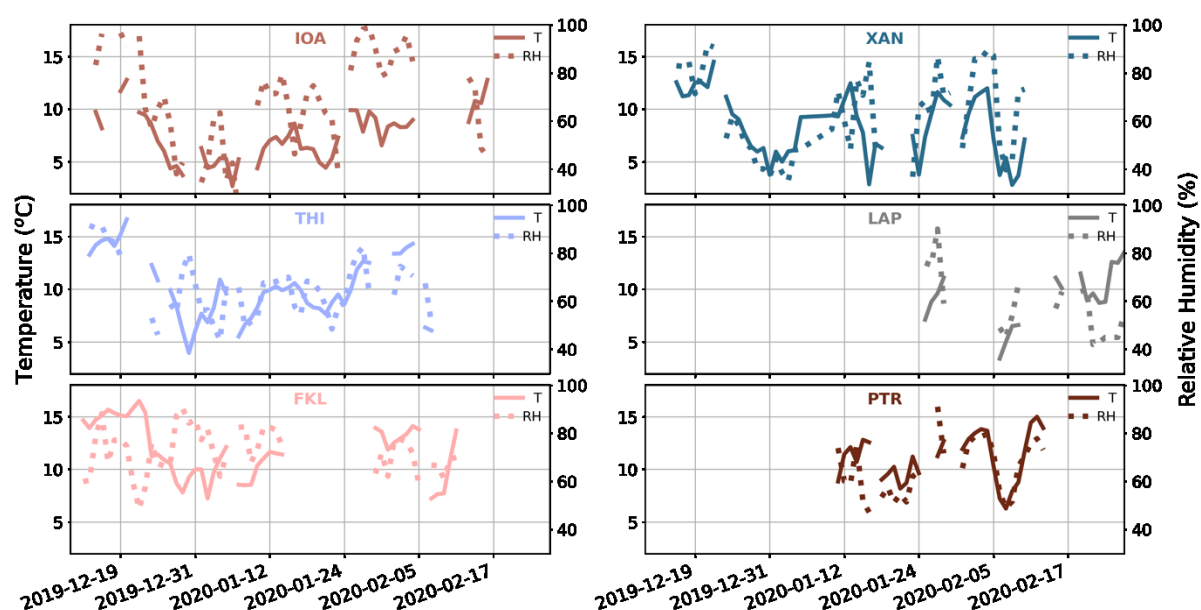

Figure S1: Timeseries of Temperature (left y axis, solid lines) and Relative Humidity (right y axis, dashed lines) for IOA, XAN, THI, LAP, FKL and PTR during winter 2019-2020.
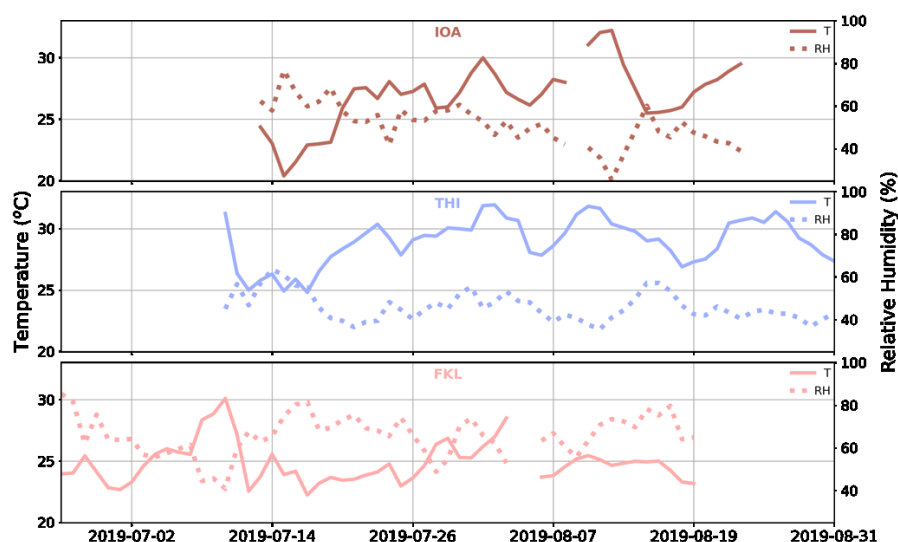
Figure S2: Timeseries of Temperature (left y axis, solid lines) and Relative Humidity (right y axis, dashed lines) for IOA, THI and FKL during summer 2019.

A3. Evaluation of aerosol pH derived from ISORROPIA-lite

For the evaluation of the model we focused mainly on the case of PTR (Fig. 4, main text), since it was the only site with available NH_3 measurements. Nevertheless, gas phase HNO_3 observations were not available for the studied period and for this we used the most recent HNO_3 measurements near the site (THI), an average value of 0.53 ± 0.12 µg/m^3 in winter from 12/2014 to 3/2016. An earlier study conducted at PTR reported a HNO_3 concentration of 1.2 µg/m^3 for January 1994 (Danalatos et al., 1995). Since HNO_3 plays an important role in aerosol pH, a sensitivity test was conducted using this level of nitric acid in our calculations. The underestimation in the partitioning of NH_4^+ (Fig. 4, main text) seems to decrease when the higher HNO_3 concentrations observed in 1994 are used (Fig. S3). In addition, the underestimation of $\varepsilon(NH_4^+)$ that was originally observed, might be associated with an overestimation of aerosol pH at PTR. The result of this sensitivity test shows indeed an average decrease in aerosol pH of about 0.2 pH units, when higher HNO_3 levels are used that also lead to higher NH_4^+.
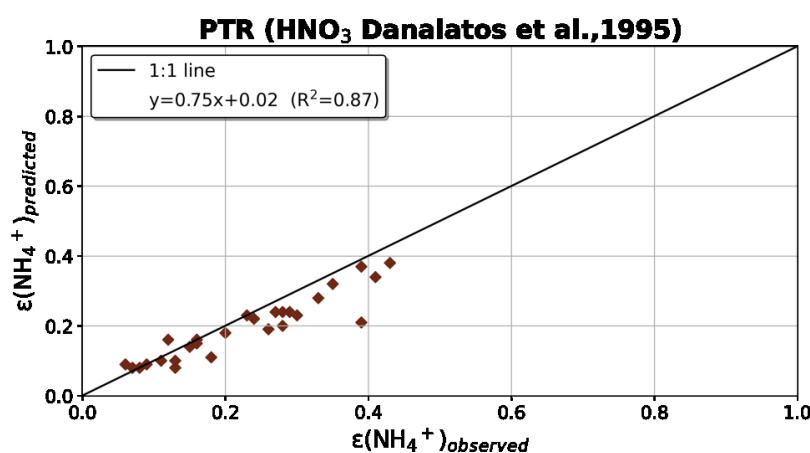

Figure S3: Evaluation of the ISORROPIA-lite results for the case of PTR using higher concentrations of HNO_3 (1.2 µg/m^3) in our calculations: Comparison of the partitioning coefficient of NH_4^+ calculated using the NH_3 and NH_4^+ observations with that using the predicted concentrations derived from the ISORROPIA model. ($\varepsilon(NH_4^+) = NH_4^+/(NH_4^+ + NH_3)$).
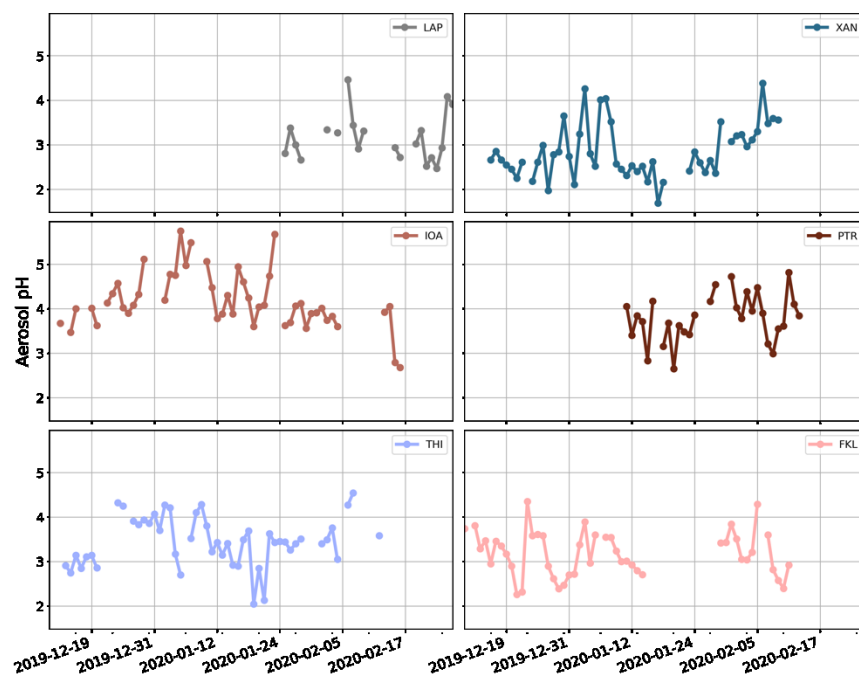
A4. Inorganic aerosol pH

Figure S4: Variation of the fine aerosol pH accounting only for the inorganics as derived from ISORROPIA-lite for LAP, XAN, IOA, PTR, THI and FKL for winter 2019-2020.
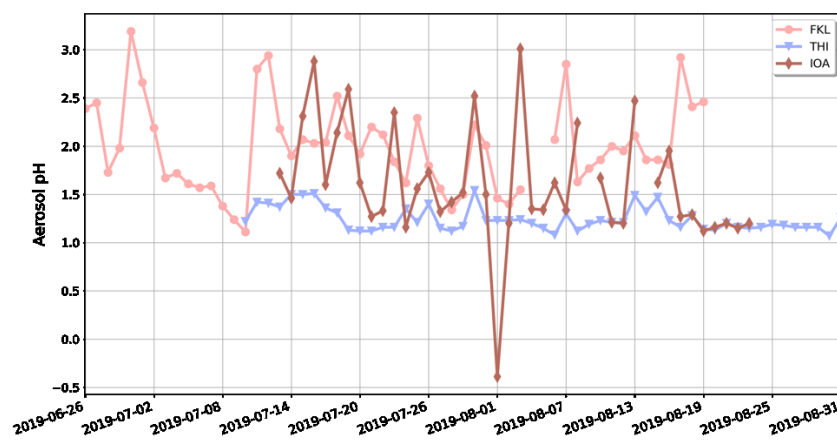

Figure S5: Variation of the pH of fine aerosol accounting only for the inorganic aerosol components as derived from ISORROPIA-lite for IOA, THI and FKL for summer 2019.

Table S2: Multiple linear regression of the aerosol pH as derived from ISORROPIA-lite during winter 2019-2020 with the variables used as inputs. The total R^2 is derived from the regression using all variables and the R^2 reported for each variable is the coefficient resulting from the exclusion of this variable from the regression. The contribution to R^2 is the reduction in the coefficient divided by the total one and expressed in percentage. The initial p-value is the p-value from the regression using all variables (significance level, 0.05).

		T	RH	Na^+	SO_4^{2-}	TNH_3	TNO_3	Cl^-	Ca^{2+}	K^+	Mg^{2+}	OA
FKL Total R^2 = 0.79	R^2	0.79	0.75	0.74	0.54	0.77	0.79	0.79	0.78	0.78	0.79	0.76
	Contribution to R^2 (%)	0.94	5.13	6.67	32.08	2.46	-0.02	0.03	1.45	1.14	0.54	4.82
	Initial p-value	0.27	0.01	0.01	0.00	0.08	0.99	0.79	0.17	0.23	0.39	0.02
THI Total R^2 = 0.82	R^2	0.79	0.80	0.82	0.48	0.71	0.82	0.82	0.80	0.82	0.80	0.82
	Contribution to R^2 (%)	4.68	2.91	0.84	41.56	14.12	0.19	0.06	2.36	0.07	2.70	0.02
	Initial p-value	0.01	0.03	0.24	0.00	0.00	0.58	0.77	0.05	0.74	0.04	0.87
PTR Total R^2 = 0.84	R^2	0.83	0.83	0.74	0.72	0.82	0.83	0.84	0.82	0.76	0.83	0.84
	Contribution to R^2 (%)	1.16	1.57	12.49	13.85	2.41	1.34	0.38	2.79	9.09	1.18	0.14
	Initial p-value	0.33	0.26	0.00	0.00	0.17	0.30	0.59	0.14	0.01	0.33	0.77
IOA Total R^2 = 0.48	R^2	0.46	0.48	0.47	0.38	0.43	0.43	0.45	0.39	0.46	0.48	0.47
	Contribution to R^2 (%)	3.76	0.13	2.46	20.63	9.39	11.40	5.91	19.28	4.57	0.41	1.99
	Initial p-value	0.28	0.90	0.38	0.01	0.09	0.06	0.17	0.02	0.23	0.74	0.43
LAP Total R^2 = 0.74	R^2	0.74	0.72	0.48	0.50	0.54	0.74	0.70	0.65	0.70	0.71	0.71
	Contribution to R^2 (%)	0.03	2.75	35.06	32.94	27.32	0.58	5.10	12.56	5.42	3.70	4.00
	Initial p-value	0.93	0.45	0.02	0.03	0.04	0.73	0.31	0.13	0.30	0.39	0.37
XAN Total R^2 = 0.70	R^2	0.64	0.69	0.70	0.43	0.56	0.70	0.69	0.69	0.70	0.70	0.70
	Contribution to R^2 (%)	9.06	1.09	0.86	39.07	19.71	0.84	2.26	1.18	0.01	0.21	0.80
	Initial p-value	0.01	0.32	0.38	0.00	0.00	0.38	0.16	0.30	0.89	0.66	0.39

Table S3: Multiple linear regression of the aerosol pH as derived from ISORROPIA-lite during summer 2019 with the variables used as inputs. The total R^2 is derived from the regression using all variables and the R^2 reported for each variable is the coefficient resulting from the exclusion of this variable from the regression. The contribution to R^2 is the reduction in the coefficient divided by the total one and expressed in percentage. The initial p-value is the p-value from the regression using all variables (significance level, 0.05).

		T	RH	Na^+	SO_4^{2-}	TNH_3	TNO_3	Cl^-	Ca^{2+}	K^+	Mg^{2+}	OA
FKL Total R^2 = 0.95	R^2	0.92	0.90	0.92	0.95	0.94	0.94	0.93	0.92	0.94	0.95	0.93
	Contribution to R^2 (%)	2.62	5.04	2.31	0.07	0.38	1.14	1.17	2.40	0.52	0.06	1.56
	Initial p-value	0.00	0.00	0.00	0.49	0.11	0.01	0.01	0.00	0.06	0.54	0.00
THI Total R^2 = 0.93	R^2	0.92	0.77	0.87	0.72	0.88	0.93	0.93	0.83	0.93	0.91	0.83
	Contribution to R^2 (%)	0.55	17.52	6.94	22.73	5.87	-0.12	0.33	11.11	0.50	2.42	10.68
	Initial p-value	0.05	0.00	0.00	0.00	0.00	0.53	0.10	0.00	0.06	0.00	0.00
IOA Total R^2 = 0.94	R^2	0.94	0.94	0.92	0.72	0.92	0.93	0.94	0.84	0.88	0.94	0.94
	Contribution to R^2 (%)	0.48	0.17	2.50	23.07	2.64	1.27	0.12	11.16	6.15	0.27	0.17
	Initial p-value	0.22	0.65	0.00	0.00	0.00	0.03	1.00	0.00	0.00	0.43	0.63

A5. Sensitivity tests

Table S4: Sensitivity test for the determination of the major contributors for the seasonal variability of aerosol pH at FKL. Simulations S_1, S_2, S_3, S_4 were done, running the model (ISORROPIA-lite) and using the wintertime observations in addition for each simulation the summer mean K^+, NH_3, SO_4^{2-} and temperature were used respectively. The ΔpH is reported as the absolute difference $pH_{winter} - pH_{winter(summerX)}$.

Initial pH (wintertime pH)	Simulations	Description of the simulation winter data with summer	Aerosol pH	absolute ΔpH
	S_1	mean K^+	3.29 ± 0.49	0.15
	S_2	mean TNH_3	3.56 ± 0.41	0.39
3.17 ± 0.48	S_3	mean SO_4^{2-}	1.51 ± 0.97	1.66
	S_4	mean Temperature	3.03 ± 0.74	0.30

Table S5: Sensitivity test for the determination of the major contributors for the seasonal variability of aerosol pH at IOA. Simulations S_1, S_2, S_3, S_4, S_5, S_6, S_7, S_8, S_9 were done, running the model (ISORROPIA-lite) and using the wintertime observations, in addition for each simulation the summer mean temperature, relative humidity, TNO_3, TNH_3, SO_4^{2-}, Na^+, K^+, Ca^{2+} and OA were used respectively. The ΔpH is reported as the absolute difference $pH_{winter} - pH_{winter(summerX)}$.

Initial pH (wintertime pH)	Simulations	Description of the simulation winter data with summer	Aerosol pH	absolute ΔpH
	S_1	mean Temperature	3.23 ± 0.34	0.76
	S_2	mean Relative Humidity	3.98 ± 0.35	0.21
	S_3	mean TNO_3	4.79 ± 1.45	0.98
	S_4	mean TNH_3	3.40 ± 0.68	0.59
3.99 ± 0.41	S_5	mean SO_4^{2-}	3.89 ± 0.91	0.45
	S_6	mean Na^+	3.94 ± 0.40	0.06
	S_7	mean K^+	3.85 ± 0.99	0.53
	S_8	mean Ca^{2+}	4.17 ± 1.01	0.43
	S_9	mean OA	4.12 ± 0.57	0.22

Table S6: Sensitivity test for the determination of the major contributors for the seasonal variability of aerosol pH at THI. Simulations S_1, S_2, S_3, S_4, S_5, S_6, S_7, S_8 were done, running the model (ISORROPIA-lite) using the wintertime observations, in addition for each simulation the summer mean temperature, relative humidity, SO_4^{2-}, K^+, Ca^{2+}, Na^+, TNH_3 and TNO_3 were used respectively. The ΔpH is reported as the absolute difference $pH_{winter} - pH_{winter(summerX)}$.

Initial pH (wintertime pH)	Simulations	Description of the simulation winter data with summer	Aerosol pH	abs ΔpH
	S_1	mean Temperature	$3.04 \pm 0.60x$	0.42
	S_2	mean Relative Humidity	3.58 ± 0.63	0.24
	S_3	mean SO_4^{2-}	0.53 ± 0.93	2.84
3.38 ± 0.51	S_4	mean K^+	3.26 ± 0.50	0.15
	S_5	mean Ca^{2+}	3.64 ± 0.98	0.33
	S_6	mean Na^+	3.33 ± 0.55	0.12
	S_7	mean TNH_3	3.86 ± 0.50	0.48
	S_8	mean TNO_3	3.37 ± 0.44	0.16

A6. Sensitivity of pH to gas phase NH_3 and HNO_3

Table S7: Sensitivity of pH estimation to gas phase NH_3 and HNO_3 concentrations. The base case concentrations of the gases are provided along with the difference in aerosol pH ($\Delta pH = pH_{x2gas} - pH_{original}$ and $\Delta pH = pH_{1/2gas} - pH_{original}$) between the simulations when double and half the amount of the gas is used and the original simulation (base case). The numbers in the parenthesis correspond to the number of days.

	FKL		THI		PTR	IOA		LAP	XAN
	January (16)	July & August (34)	January (27)	July & August (34)	January (16)	January (27)	July & August (34)	January (4)	January (26)
NH_3 (µg/m³)	1.06	1.24	0.65	1.31	2.99	2.55	1.04	0.30	0.71
ΔpH x2NH_3	0.34	0.29	0.21	0.23	0.28	0.28	0.26	0.13	0.25
ΔpH ½NH_3	-0.31	-0.24	-0.15	-0.10	-0.25	-0.26	-0.15	-0.07	-0.21
HNO_3 (µg/m³)	0.63	0.95	0.53	0.91	0.53	0.53	0.91	0.53	0.53
ΔpH x2HNO_3	-0.11	-0.01	-0.15	-0.02	-0.06	-0.06	-0.02	-0.07	-0.04
ΔpH ½HNO_3	0.08	0.01	0.15	0.05	0.07	0.05	0.03	0.04	0.03

A7. Sensitivity of $PM_{2.5}$ to gas phase NH_3 and HNO_3

Table S8: Seasonally mean values of temperature in the studied sites (all sites in winter and FKL, THI and IOA in summer) along with the mean activity coefficients ($\gamma_{H^+}\gamma_{NO_3^-}$ and $\gamma_{NH_4^+}\gamma_{NO_3^-}$) that were derived for ISORROPIA-lite and used in the Nenes et al. (2020) framework. The aerosol pH and water used in the framework are also presented here, as mean values for each season.

Season	Temperature (°C)	$\gamma_{H^+}\gamma_{NO_3^-}$	$\gamma_{NH_4^+}\gamma_{NO_3^-}$	Aerosol pH	Aerosol water (µg/m³)
winter (Jan)	9.06 ± 1.83	0.64 ± 0.25	0.20 ± 0.06	3.41 ± 0.52	7.78 ± 8.63
summer (Jul-Aug)	26.69 ± 1.99	0.27 ± 0.03	0.23 ± 0.02	1.64 ± 0.38	3.07 ± 1.62

A8. Partitioning coefficient of nitrate during winter and summer

The gas-particle partitioning coefficient of nitrate was calculated using the results derived from ISORROPIA-lite for all sites during winter and summer considering both simulations: the one when only the inorganic species are participating in the system and the other when the organics area also added. The addition of the organics resulted in a slight increase of the partitioning of nitrate since the presence of the organics raise the total aerosol water content which in turn favors the partitioning of nitrate to the aerosol phase.

When comparing the partitioning coefficient between the seasons, in regions where the variation of aerosol acidity was prominent i.e. in IOA (2 pH units more acidic particles were present in summer than in winter) and FKL (1 pH unit higher aerosol pH in winter than in summer) the resulted seasonal difference in the partitioning of nitrate is also distinct. The more acidic conditions at both sites during summer caused nitrate to reside more to the gas phase. Similarly, during summer particle phase nitrate at THI was not present in contrast to winter were the moderate aerosol acidity allowed the partitioning of nitrate to the aerosol phase.
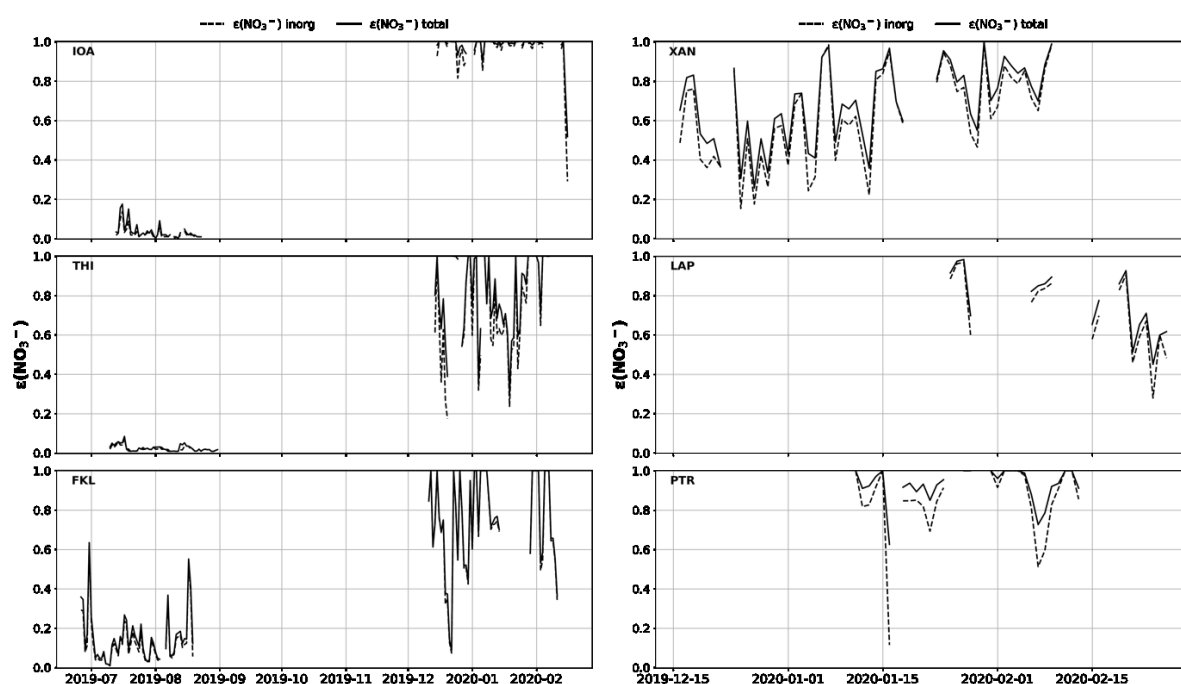

Figure S6: Timeseries of the gas-to-particle partitioning coefficient (daily values) calculated as $\varepsilon(NO_3^-) = NO_3^-/(NO_3^- + HNO_3)$ as derived from ISORROPIA-lite for all sites during summer and winter (where applicable i.e. summer data only available in IOA, THI and FKL). With dashed lines the $\varepsilon(NO_3^-)$ is reported using the results from the model considering only the inorganic pollutants while with solid lines the results when accounting also for the organics are shown. When $\varepsilon(NO_3^-)$ is equal to 1, all nitrate is partitioning in the aerosol phase; while for $\varepsilon(NO_3^-)$ close to zero, the partitioning is to the gas phase as HNO_3.

References

Danalatos, D., Glavas, S., and Kambezidis, H.: Atmospheric nitric acid concentrations in a Mediterranean site, Patras, Greece, Atmospheric Environment, 29, 1849–1852, https://doi.org/10.1016/1352-2310(95)00061-3, 1995.

Miller, J. N. and Miller, J. C.: Statistics and chemometrics for analytical chemistry, 6th ed., Prentice Hall/Pearson, Harlow, 2010.